Soil Biology & Biochemistry 85 (2015) 82–88

Contents lists available at ScienceDirect

Soil Biology & Biochemistry

journal homepage: www.elsevier.com/locate/soilbio

Nanoscale evidence of contrasted processes for root-derived organic matter stabilization by mineral interactions depending on soil depth

Cornelia Rumpel [a, *], Karen Baumann [a, 1], Laurent Remusat [b], Marie-France Dignac [a], Pierre Barré [c], Damien Deldicque [c], Gunnar Glasser [d], Ingo Lieberwirth [d], Abad Chabbi [a, e]

[a] CNRS, IEES, UMR CNRS-INRA-UPMC-UPEC-IRD-ParisAgroTech, Campus ParisAgroTech, Thiverval-Grignon, France
[b] IMPMC, UMR CNRS 7590, Sorbonne Universités, MNHN, UPMC, IRD, CP 52 – 57 rue Cuvier, 75231 Paris Cedex 05, France
[c] CNRS, ENS Geologie, Paris, France
[d] Max Planck Institute for Polymer Research, Mainz, Germany
[e] INRA, UR P3F, Centre INRA Poitou-Charentes, Lusignan, France

ARTICLE INFO

Article history:
Received 8 September 2014
Received in revised form
5 February 2015
Accepted 16 February 2015
Available online 4 March 2015

Keywords:
Organic matter stabilization
Subsoil
Organo-mineral interactions
Metal oxides NanoSIMS

ABSTRACT

Up to now stabilization of organic matter (OM) in soils due to mineral interactions has been assessed mainly by correlations between carbon and iron and/or aluminum oxides evidencing that metal oxides may be principal stabilization agents. The nature and morphology of stabilized OM are poorly known. Taking advantage of a field experiment, the aim of our study was to analyze the fate of ^{13}C and ^{15}N labeled root material at 30 and 90 cm depths after three years of incubation and to characterize the nature of OM stabilized by interactions with metal oxides. Our methodological approach included isolation of metal oxides by physical fractionation and visualization of their interaction with OM using NanoSIMS. We concentrated metal oxides in a fraction corresponding to our objectives: the heavy fraction (>3 g cm^{-3}) of fine silt. NanoSIMS analyses of this fraction allowed us to locate unlabeled OM and OM either double labeled or carrying one single label in association with metal oxides. Our results suggest that decoupling of C and N may have happened during OM stabilization within the timeframe of the 3 year field experiment. Scanning electron microscopy (SEM) after NanoSIMS analyzes, indicated that ^{15}N labeled OM at 90 cm were well-defined ovoid OM particles resembling to microbial cells in interaction with Fe, Al and Ti oxides. At 30 cm depth, OM associated with metal oxides was ^{13}C and ^{15}N labeled unstructured material, possibly derived from plant debris. We suggest that at the two soil depths under investigation different processes might be at work, leading to association of OM with mineral compounds of the isolated fraction: in upper soil layers, decomposed plant material may directly interact with metal oxides, whereas in deep mineral soil, OM could mainly interact with metal oxides after microbial turnover. Both types of interactions may be fairly stable as they persisted after ultrasonication and salt extraction.

1. Introduction

Soil organic matter (SOM) stability is governed by accessibility rather than recalcitrance (Dungait et al., 2012). In particular, interaction with the mineral phase was identified as the only mechanism able to stabilize a significant proportion of SOM for long timescales by adsorption of OM onto Fe and Al oxides (Kögel-Knabner et al., 2008). These processes were made responsible for the extremely long residence times of OM stored in subsoil horizons (Eusterhues et al., 2003; Kleber et al., 2005). The nature of mineral interactions has long been discussed and SOM adsorption was hypothesized to occur as monolayer equivalent (Mayer, 1994) as well as patchy distribution (Ransom et al., 1998; Vogel et al., 2014). The composition of SOM stabilized by mineral interactions has also been a matter of debate up to date: while aromatic lignin molecules were found to be preferentially sorbed onto metal oxides (Kaiser and Zech, 1998; Kramer et al., 2012), other studies showed no correlation between lignin and Fe oxides in subsoil horizons (Spielvogel et al., 2008). The absence of lignin stabilization through

* Corresponding author. Tel.: +33 1 30 81 54 79; fax: +33 1 30 81 54 97.
E-mail address: cornelia.rumpel@grignon.inra.fr (C. Rumpel).
[1] Current address: Institute for Land Use, Faculty for Agriculture and Environmental Sciences, Rostock University, Rostock, Germany.

http://dx.doi.org/10.1016/j.soilbio.2015.02.017
0038-0717/

mineral interactions was recently hypothesized to be a methodological artifact (Hernes et al., 2013). Easily available polysaccharides are stabilized by the mineral phase in top- (Kiem and Kögel-Knabner, 2003) and subsoil horizons (Liang and Balser, 2008, Rumpel et al., 2010). A recent theory postulates the adsorption of nitrogen rich material onto mineral surfaces (Kleber et al., 2007), suggesting that in particular microbial material would be stabilized by interaction with the mineral phase. This is in agreement with recent findings on the importance of microbial material for SOM formation (Miltner et al., 2012). However, the nature of OM interacting with the mineral phase may depend on soil depth, since the nature of mineral-associated OM was found to be different in top- and subsoil horizons, with plant-derived compounds prevailing in topsoil and microbial material dominating in subsoil (Rumpel et al., 2012). All these findings are mainly based on statistical relationships between C and dense particles as well as Fe- and/or Al-oxides. Few studies were carried out to directly show these interactions.

This is mainly due to the fact that interaction between OM and the mineral phase of soil takes place at much finer scales than those studied in general. Due to technical limitations, the micrometer-scale complexity of soil has been rarely addressed up to date although organo-mineral interactions occur at these scales. With the development of nanoscale techniques, such as nanoscale secondary-ion mass spectrometry (NanoSIMS), the observation of organo-mineral interactions has become possible (Herrmann et al., 2007). NanoSIMS was developed to enable the differentiation between several stable isotopes at high mass resolving power and at high lateral resolution. The technique provides isotopic maps in addition to elemental maps. It allows therefore the tracking of labeled compounds and elucidating nano-scale interaction between OM and clay as well as iron oxides. For example, Mueller et al. (2012) used NanoSIMS to show heterogeneous utilization of ^{13}C and ^{15}N labeled proteins by microorganisms located on aggregate surfaces. So far most studies using NanoSIMS have been carried out in the laboratory with model compounds (e.g. Liu et al., 2013) or after laboratory incubation with natural organic material (Keiluweit et al., 2012; Vogel et al., 2014). These studies indicated patchy distribution of OM on mineral surfaces, with preferential adsorption of new OM to pre-existing organo-mineral clusters (Vogel et al., 2014). Recently, Remusat et al. (2012) used NanoSIMS *in situ* to image intact soil particles and to detect spots of isotopic enrichment a decade after ^{15}N litter labeling. They concluded preservation of OM after microbial processing through interaction with the mineral phase. By using Scanning transmission X-ray microscopy in addition to NanoSIMS, they were able to show that the organic compounds consisted of microbial products, which may include microbial cells as well as extracellular polymeric substances (Remusat et al., 2012). The protein fraction of extracellular polymeric substances was found to be sorbed preferentially on Al as well as Fe oxides (Mikutta et al., 2011; Keiluweit et al., 2012; Liu et al., 2013). However, it was also shown that sorption affects only minor parts of the extracellular polymeric substances (Liu et al., 2013).

In this study, we went a step further in the characterization of organo-mineral complex formation *in situ*. We used NanoSIMS in combination with scanning electron microscopy (SEM) to investigate the morphology of labeled OM in association with metal oxides after three years of field incubation of ^{13}C and ^{15}N labeled root litter. This experiment, in which labeled root material was mixed with soil and exposed in litterbags at different soil depths, was carried out to investigate the influence of depth on decomposition and stabilization of root litter. We observed contrasting decomposition dynamics in the different soil depths with a lag-phase occurring in deep soil (Sanaullah et al., 2011). However, in contrast to our expectations, the magnitude of root litter decomposition and stabilization was similar after 3 years at 30 and 90 cm depth (Sanaullah et al., 2011), which was in line with the similar temperature and water contents recorded at both soil depths (Sanaullah et al., 2011).

A major proportion of the remaining labeled ^{13}C and ^{15}N (about 40% of initial) was contained after 3 years in the heavy fraction (>1.8 g cm^{-3}) <50 μm (Sanaullah et al., 2011), being composed of organic matter stabilized by mineral interactions (Schrumpf et al., 2013). We hypothesized that labeled organic compounds are stabilized in this fraction due to association with Fe or Al oxides, which were shown to be the main stabilizing agents in the investigated soil (Moni et al., 2010). Moreover, we hypothesized that the nature of compounds associated with these minerals differs at 30 and 90 cm depth. In order to obtain a soil fraction containing Fe and Al oxides, we isolated the >3 g cm^{-3} fraction from fine silt by density fractionation. For elemental distribution and to identify regions of interest (ROI) the material in this fraction was analyzed by scanning electron microscopy (SEM) prior to NanoSIMS. NanoSIMS analyses were carried out to determine locations of labeled ^{13}C and ^{15}N. After NanoSIMS analyzes, we characterized the morphology and isotopic composition of the OM by SEM. The aims of the study were to.

- Demonstrate stabilization of SOM by interaction with Fe and Al oxides at different soil depths by studying one specific physical fraction
- Investigate if such a stabilization occurs within the timeframe of the field experiment
- Determine if stabilized compounds differ in contrasting depths of the soil profile

2. Materials and methods

2.1. Field incubation

The field incubation was carried out during three years at Lusignan (France) in a Cambisol soil with loamy texture (Chabbi et al., 2009) and grassland vegetation. Briefly, soil cores were excavated by an auger sampler (Ø 7.5 cm) from 30 to 90 cm depth, corresponding to well defined pedogenic horizons, i.e. A (ploughing horizon) and B2 (horizon containing red clay). Thereafter, we prepared litterbags containing labeled root material and soil from the two different soil depths. Root material was isolated from labeled wheat, which had been grown hydroponically in a growth chamber under 2 atom% $^{13}C{-}CO_2$ atmosphere with a nutrient solution containing $^{15}NH_4^{15}NO_3$ (10% ^{15}N atom excess) for 16 weeks. After harvest, the roots had been dried at 40 °C before 2 g were cut into 1 cm pieces and mixed with 100 g of soil. The soil root mixture was put in 10 × 10 cm litter bags (mesh size 100 μm), placed at the original soil depth and covered with material from the original soil core. During the experiment the site was managed as grassland, including regular cutting as well as N fertilization. After 36 months of incubation, the litterbags were retrieved and the material inside was air-dried. Total as well as labeled C showed little variation especially in the stable isotope content between the three field replicates. Therefore, one sample of each depth was used for this study for further analyses. The experimental scheme used in this study is presented in Fig. 1.

2.2. Bulk soil analyzes

The organic carbon (OC), nitrogen (N) and stable isotope (^{13}C and ^{15}N) content of bulk soil, and the fraction <50 μm were measured in a single analysis using a CHN auto-analyzer (CHN NA

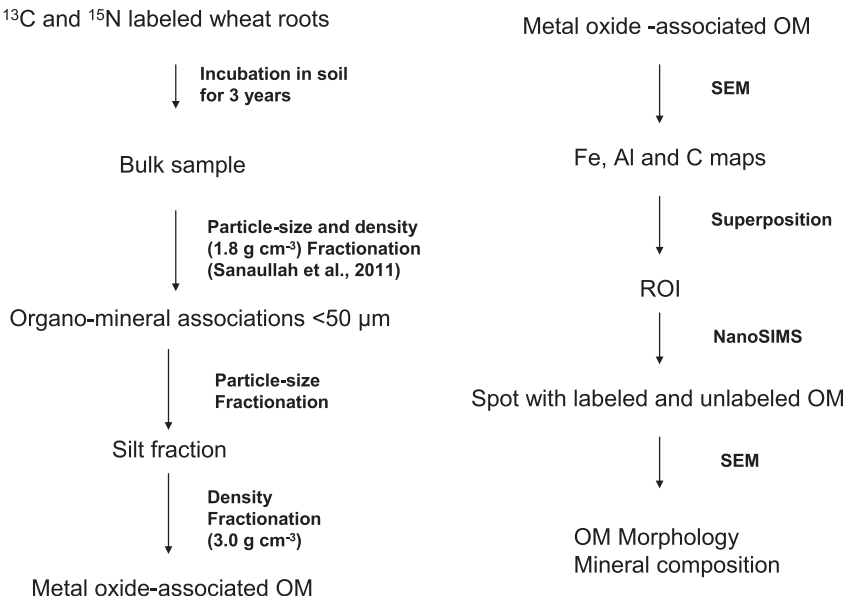

Fig. 1. Experimental scheme.

1500, Carlo Erba) coupled with an isotope ratio mass spectrometer (Optima, Elementar). Carbon and nitrogen isotope ratios were expressed in parts per thousand (‰) by using the delta notation. The isotopic ratios were calculated relative to the Pee Dee Belemnite Standard (PDB) for C and relative to atmospheric N_2 for nitrogen.

2.3. Isolation of a fraction containing Fe and Al oxides

For NanoSIMS analyzes we isolated SOM associated to metal oxides by density fractionation from the fine silt (2–6.3 µm, Fig. 1), which is the most appropriate fraction for NanoSIMS analyses according to our objectives. We intended to study the formation of organo-metal oxide interactions. These affect plant as well as microbial material. While partly decomposed plant material is generally found in the silt fraction, the clay fraction contains microbial material (Baldock et al., 1997). We chose the fine silt fraction, being at the clay/silt interface because we hypothesized that it contains organo-metal oxide associations comprising most likely decomposed root residues as well as microbial material. In order to recover fine silt, we fractionated 9 g of soil by a combination of wet sieving and centrifugation. To avoid OM redistribution, macroaggregates were dispersed by overnight shaking with 90 ml distilled water and 5 glass beads (Balesdent et al., 1991). Light plant material was removed by density fraction (>1.8 g cm^{-3}). The <50 µm fraction was then recovered by wet sieving and further dispersed by ultrasonication with a calibrated energy input of 320 J ml^{-1} (Schmidt et al., 1999). Thereafter, the <20 µm fraction was recovered by wet sieving before the fine silt fraction was isolated from the <20 µm fraction by two subsequent centrifugation steps. Finally, this fraction (2–6.3 µm) was recovered as a pellet after decanting the supernatant. The 2–6.3 µm fraction isolated during these steps was subjected to density fractionation (cut off 3 g cm^{-3}) afterwards in order to obtain a pure metal oxide associated SOM fraction. We used such a high density to be sure that we isolate metal oxides with OM just adsorbed to the free surface, we wanted to exclude particles containing big patches of OM in order to increase the probability to observe OM-metal interactions with the new root-derived C.

Density fractionation was carried out by adding 20 ml sodium-polytungstate with a density of 3 g cm^{-3}, re-dispersion in an ultrasonic bath for 1 h and centrifugation for 9 min at 1000 RPM. The supernatant was discarded and the density fraction >3 g cm^{-3} was recovered. This procedure was repeated three times. Thereafter the fraction was rinsed three times with 50 ml of distilled water, and freeze-dried before SEM and NanoSIMS analyses. The fine silt fraction (2–6.3 µm) represented 9% of the total soil mass, while particles with a density > 3 g cm^{-3} represented <0.5% of soil mass. The amount of bulk soil material in the litter bag collected after the 3-year field incubation was too low to allow for extracting enough dense (>3 g cm^{-3}) fine silt (2–6.3 µm) material for subsequent stable isotope (^{13}C and ^{15}N) determination on the bulk fraction.

2.4. Scanning electron microscopy (SEM)

Prior to visualization of organo-metal oxide interactions with NanoSIMS, we used SEM (Fig. 1), to identify regions of interest (ROI). Distilled water was added to the sample and an aliquot of the suspension was put on a Si_3N_4 wafer without any sputtering. Scanning electron microscopy was carried out using a Hitachi SU 8000 electron microscope equipped with an EDX analyzer (Bruker AXS XFlash Detector 5010). We recorded elemental as well as heatmaps for Fe, Al and C. The ROIs were identified by superposing these maps. We focused NanoSIMS imaging on ROIs showing co-localization of Fe and/or Al and C (Fig. 2). We identified 14–16 ROI for each sample.

2.5. NanoSIMS

Prior to NanoSIMS analyzes the samples were gold coated (20 nm thick) to improve lateral charge compensation. NanoSIMS analyses were carried out on the Cameca (Gennevilliers, France) NanoSIMS 50 installed at the MNHN in Paris. We used a 16 keV primary Cs^+ beam to collect secondary ions of $^{12}C^-$, $^{13}C^-$, $^{16}O^-$, $^{26}CN^-$, $^{27}CN^-$ in multicollection mode. The primary beam was set to 3 pA, leading to a spatial resolution of about 150 nm. We collected 256 × 256 pixel images covering 20 × 20 μm^2 with a raster speed of 2 ms/pix. Prior to each analysis, we used a 400 pA primary current for presputtering 25 × 25 μm^2 surface area during 6 min; this was performed to remove coating, clean the surface, and reach the sputtering steady state (Thomen et al., 2014). We used Hamamatsu discrete dynode electron multipliers with a dead time of 44 ns. We

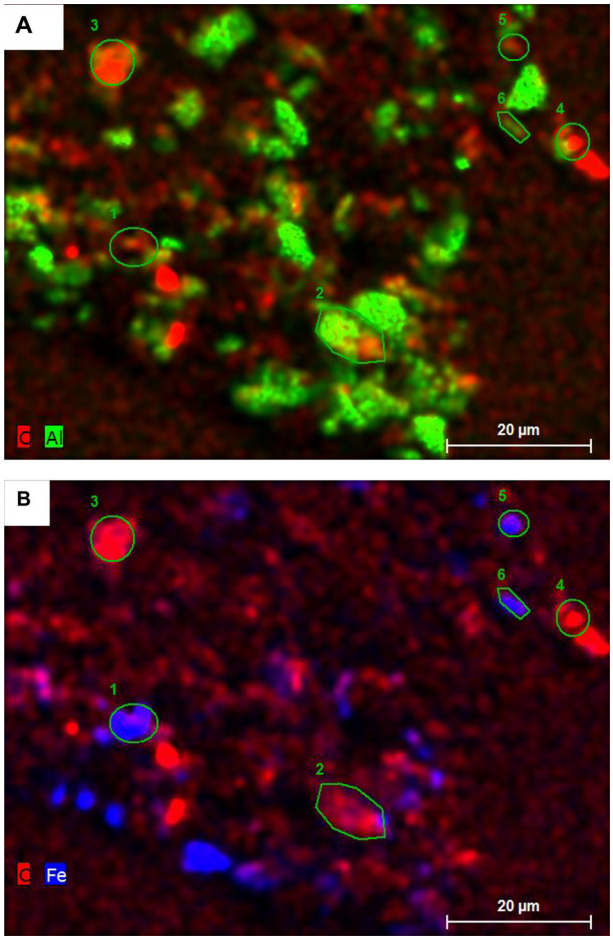

Fig. 2. Elemental maps recorded by SEM before NanoSIMS showing the distribution of C and Al (A), C and Fe (B) and the identified regions of interest.

set the mass spectrometer to a mass resolving power of 8000 to be able to resolve potential mass interferences including $^{12}C^{15}N^-$ from $^{13}C^{14}N^-$. To improve charge compensation, we used the electron-flooding gun of the NanoSIMS. During the session the vacuum did not exceed 3×10^{-10} torr. A type 3 kerogen and a charcoal were used as standards to check for stability over the session and determine the instrumental mass fractionation. All NanoSIMS images were processed with limage software developed by Larry Nittler (Carnegie Institution in Washington DC, USA). Each image being a stack of multiple frames, the first step consists in aligning each frame using a correlation algorithm and applying the same shift in X and Y to all the pixels of a single frame. Then, ratio images could be generated. For each analysis, 30 planes were accumulated (66 min long analysis for 20 by 20 microns). The isotopic ratios were calculated using the total counts recorded for C- and CN- ions for C and N isotopic ratios, respectively. Instrumental bias on the isotopic ratios was corrected using terrestrial standards of known composition. Delta values reported in the manuscript and the figures are therefore delta values vs the international references (PDB or Air).

3. Results

3.1. C and N content of organo-mineral associations

The C and N analyzes were carried out for the <50 µm fraction (Table 1). Carbon content ranged between 3 and 7.5 mg g^{-1} and nitrogen content between 0.6 and 0.9 mg g^{-1}. Much lower values were recorded at 90 cm depth as compared to 30 cm. In deep soil, labeled C and N had 30 and 10% higher contributions to SOM than at 30 cm depth.

3.2. SEM before NanoSIMS

Using SEM, we identified regions of interest by superposition of elemental maps of Fe and Al oxides and C (Fig. 2). On the Al map, many Al containing minerals could be identified, as well as several regions containing C. The Fe map shows few iron containing minerals in the same region. We focused nanoSIMS scanning on regions of interest (ROI) showing co-localization of Fe and/or Al and C.

3.3. NanoSIMS analyzes

Fig. 3 shows two representative examples of NanoSIMS maps of C (^{12}C and ^{13}C), N (^{14}N and ^{15}N), and O (^{18}O). We observed OM spots with correlated ^{13}C and ^{15}N enrichment (Fig. 3a) and OM spots showing ^{15}N enrichment, while C was showing natural abundance contents of ^{13}C (Fig. 3b). In addition we observed spots showing natural abundance of ^{13}C and ^{15}N.

Table 2 shows the total number of spots analyzed by NanoSIMS as well as a visual apprehension of their isotopic composition. In total we analyzed 29 spots in the ROIs for the sample taken at 30 cm and 24 spots for the samples taken at 90 cm depth. At 30 cm depth, 48% of the spots carried the ^{13}C as well as the ^{15}N label. While unlabeled spots had similar contribution to both depths only one spot at 30 cm depth was solely ^{13}C labeled. Higher occurrence was noted for spots carrying exclusively the ^{15}N label. At 90 cm depth, these spots contributed to about one third of the particles (Table 2).

The location of OM spots observed with NanoSIMS on the Fe maps obtained with SEM are depicted in Fig. 4. This figure shows that unlabeled as well as labeled C and N compounds were not found in all cases in close association with Fe (Fig. 4) and/or Al oxides (data not shown). In order to identify the minerals involved in OM-metal oxide associations we went back to SEM.

3.4. SEM after NanoSIMS

Identification of ROI analyzed by NanoSIMS under SEM was easy, since the Cs beam had led to abrasion of Au coating the sample surface. Within one ROI, it was also easy to clearly identify the organic particles observed before with NanoSIMS, because they presented traces of abrasion created by the Cs beam in pure SOM. The SEM images recorded after NanoSIM showed for all samples from subsoil at 90 cm depth, that the OM analyzed by NanoSIMS had an ovoid morphology with a size of 500–1000 nm (Fig. 5). These well-defined ovoid OM particles resembled to microbial cells attached to minerals, but more advanced techniques would be needed to confirm this. In the ROI of the samples taken at 30 cm depth we were not able to observe such structures. Organic matter particles, which underwent NanoSIMS analyzes, were bigger (around 2 µm) unstructured and mixed within the mineral phase

Table 1
General parameters of the <50 µm fraction after 3 years of incubation with ^{13}C and ^{15}N labeled root material.

Depth	<50 µm fraction of samples recovered after 3 years of incubation				
	C	N	^{13}C content	^{15}N content	$^{13}C/^{15}N$
	mg g^{-1}	mg g^{-1}	mg g^{-1}	mg g^{-1}	
30 cm	7.56 ± 0.35	0.95 ± 0.05	0.70 ± 0.02	0.05 ± 0.00	14
90 cm	3.18 ± 0.15	0.63 ± 0.02	0.88 ± 0.08	0.07 ± 0.01	12

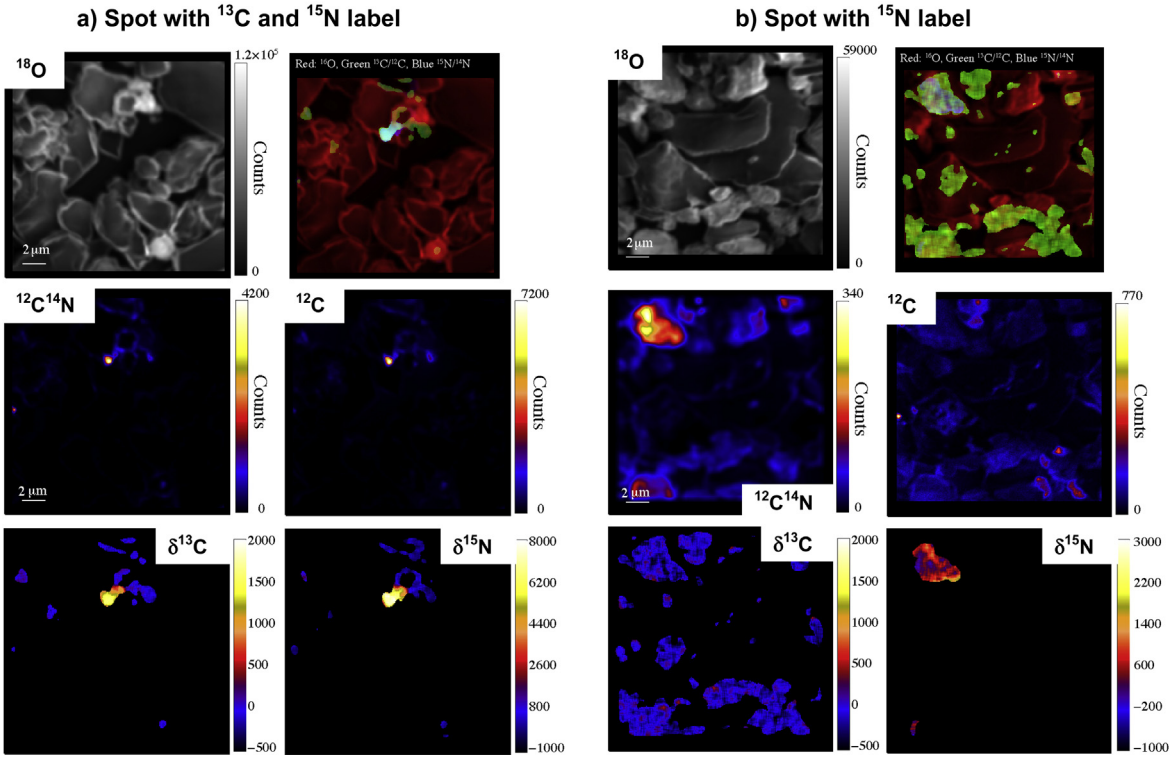

Fig. 3. Maps of the distribution of ^{16}O, ^{12}C, ^{13}C, ^{14}N and ^{15}N obtained by NanoSIMS analyses of the > 3 g cm^{-3} fraction for two spots.

(Fig. 5). The minerals in interaction with SOM were identified as Fe–Al–Ti mixed phases.

4. Discussion

4.1. Amount of mineral associated SOM and root C and N contribution to the <50 µm fraction in 30 and 90 cm depth

The C and N data of the <50 µm fraction isolated after density fractionation (density cutoff 1.8 g cm^{-3}, Sanaullah et al., 2011) after 3 years of root litter incubation show that new root derived C may constitute between 9% and 27% of mineral-associated organic C at 30 and 90 cm depth, while root derived N represented between 6% and 11% of mineral-associated N (Table 1). This indicates that at both depths organo-mineral associations were formed with new root derived OM during the three year experiment. In subsoil, new root C makes up higher proportions of mineral associated C (Table 1) probably due to the lower C saturation of mineral surfaces as compared to topsoil and the higher amounts of reactive metal oxides (Moni et al., 2010). This is in agreement with observations that mineral associated C contributes in higher proportion to SOM in subsoil as compared to topsoil (Rumpel and Kögel-Knabner, 2011). The $^{13}C/^{15}N$ ratio of SOM in the <50 µm fraction was wider in 30 cm depth than 90 cm. This indicates greater enrichment of N compared to C in deep soil and hence probably more intensive transformations during the process of root-derived C and N association with the mineral phase. This hypothesis is in agreement with correlations between biomarkers and mineral associated OM indicating that mineral associated SOM in subsoils contains higher proportions of microbial material than in topsoils (Liang and Balser, 2008; Rumpel et al., 2010). In order to better apprehend the OM types and minerals, in particular the metal oxides implicated in OM interactions, we subjected the >3 g cm^{-3} fraction of fine silt to SEM and NanoSIMS analyses.

Table 2
Contribution of label in spots of both soil depths analysed with NanoSIMS.

Depth	$^{12}C^{14}N$	$^{12}C^{15}N$	$^{13}C^{15}N$	$^{13}C^{14}N$	Total
	%	%	%	%	
30 cm	31	21	48	0	29
90 cm	33	29	33	4	24

4.2. Isotopic signature and morphology of stabilized OM at two different soil depths and their implication for C stabilization

NanoSIMS analyses allows for obtaining elemental and isotopic information on mineral associated OM at a very small scale, of which the composition may not be representative for the whole soil sample. However, this kind of analyses is necessary to understand the actual processes involved in the formation of organomineral associations, which operate at these scales and which are important for soil C sequestration. In this study, we wanted to address the timescale and OM compounds implicated in metal oxide-OM associations. Therefore, we applied an experimental scheme designed to analyze Fe and Al oxides containing mostly mineral surfaces with little OM association (Fig. 1). On such surfaces we expected association with new labeled root-derived OM. We chose the ROI according to Al, Fe and C co-location on SEM elemental maps in agreement with our hypothesis. Ultimately the C-metal oxide interactions we analyzed are specific and may not be representative for all OM-metal associations occurring within the soil sample. We excluded especially C-metal oxide associations with higher OM loadings. However, the information we obtained by our analyses may be very relevant process information concerning the timescale, soil depth, and elements involved in the formation of these associations.

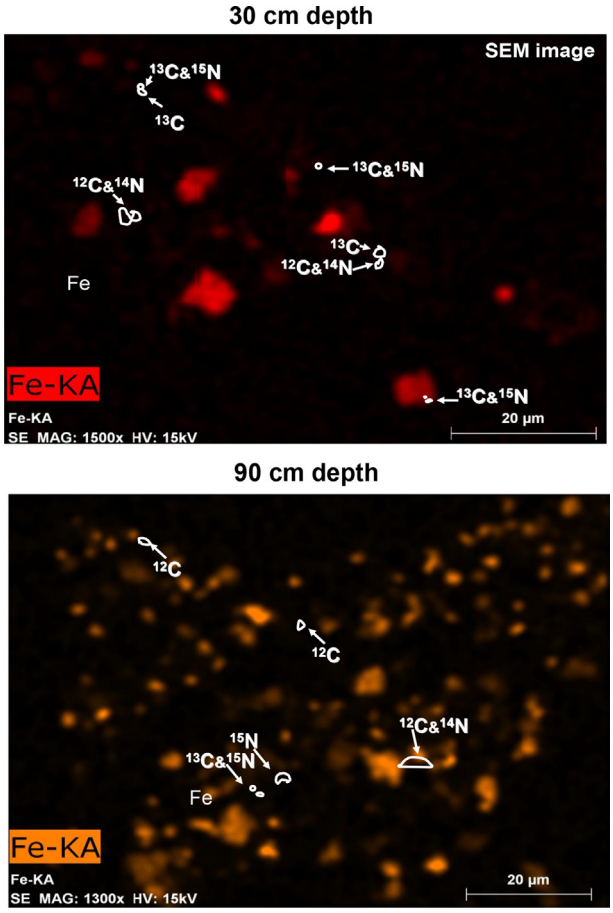

Fig. 4. Location of labeled and unlabeled C and N compounds identified by NanoSIMS on Fe maps generated by SEM.

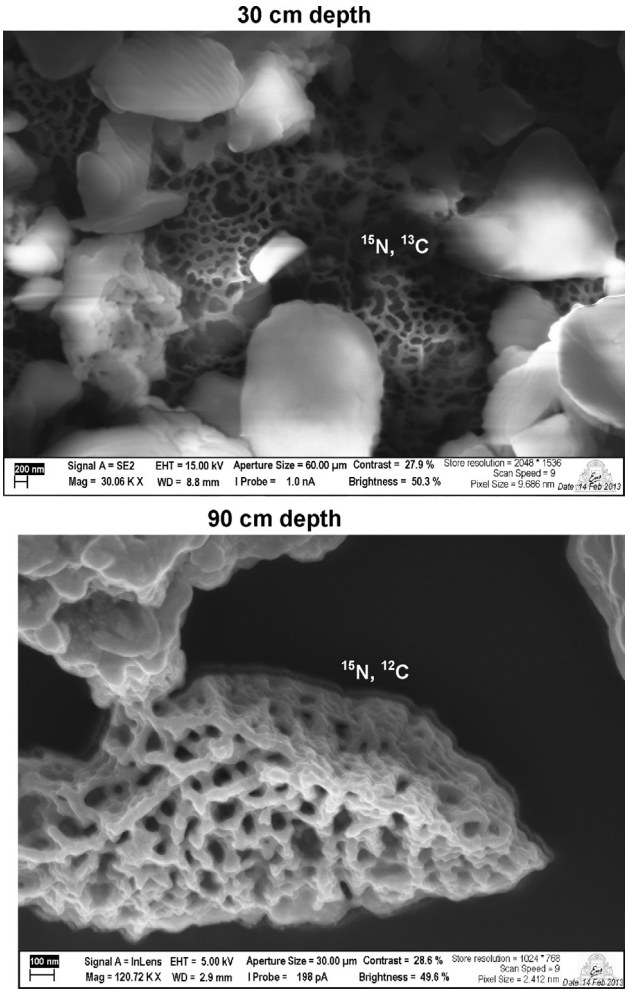

Fig. 5. Morphology of organic matter in association with mineral particles analysed by SEM after NanoSIMS analyses. Note, that the organic particles in contrast to the mineral ones show damage due to the Cs beam.

Previous quantitative assessment of root degradation and stabilization in bulk soil indicated that after three years similar amounts of root material remained and contributed to C comprised in the <50 µm fraction at both soil depths and is thus potentially associated with soil minerals (Sanaullah et al., 2011, Fig. 6, Table 1). In the >3 g.cm^{-3} fraction of fine silt, which may contain exclusively OM associated to metal oxides, we found unlabeled SOM, ^{13}C and ^{15}N labeled SOM (Fig. 3a) and solely ^{15}N labeled SOM (Fig. 3b). At both depths a greater proportion of particles contained exclusively the ^{15}N label (Fig. 3b; Table 2). The occurrence of ^{15}N only labeled spots was greater at 90 cm compared to 30 cm (Table 2). Thus our study demonstrates that organo-mineral interactions of root litter and metal oxides were formed within the three years time frame of the field experiment. Our data are in contrast to results from short term incubation experiments, which indicated joint association of new C and N with minerals after 42 days (Vogel et al., 2014). They could indicate that decoupling of C and N happens in the long run and may occur in deep soil to a greater extent than at lower depths.

Location of labeled spots on Fe and Al maps indicated that Al and Fe oxides do not seem to be the principal minerals implicated in organo-metal oxide associations at both depths (Fig. 4). SEM analyses after NanoSIMS showed that the minerals implicated consisted of Fe/Al/Ti mixed phases. This is in accordance with mineral characterization of the >2.6 g cm^{-3} fraction isolated from bulk soil (Basile-Doelsch et al., 2007).

When we re-analyzed the morphology of 5 random spots of each of the samples with SEM, our observations showed contrasting morphologies depending on sampling depth (Fig. 5). We observed many ovoid structures resembling microbial cells attached to minerals at 90 cm, whereas at 30 cm depth diffuse unstructured material probably plant-derived OM dominated (Fig. 5). This could indicate in agreement with the elemental data for the <50 µm fraction (Table 1) that at 90 cm depth microbial biomass recycles N to a higher extent than at 30 cm depth, where the morphology of particles as well as the important presence of ^{13}C in addition to ^{15}N suggests that the degradation of the labeled root material could be less complete than at 90 cm depth. The SEM observations after NanoSIMS are in line with studies showing that microbial derived compounds contribute substantially to OM stabilized by metal oxide interactions in subsoil horizons, whereas in topsoil higher contribution of plant derived compounds were observed (Spielvogel et al., 2008). Our results could indicate that the microbial decomposition processes may be different at contrasting soil depths leading to contrasting nature of OM stabilized by metal oxide interactions. We suggest, that plant derived lignocellulosic material may be preserved by metal oxide interactions at 30 cm depth given its incomplete degradation, thereby leading to the formation of functional groups and favoring adsorption to soil minerals. This is consistent with the higher state of lignin-degradation observed at 30 cm compared with 90 cm depth (Baumann et al., 2013). At 90 cm depth, where microorganisms are most likely energy limited (Fontaine et al., 2007), degradation of

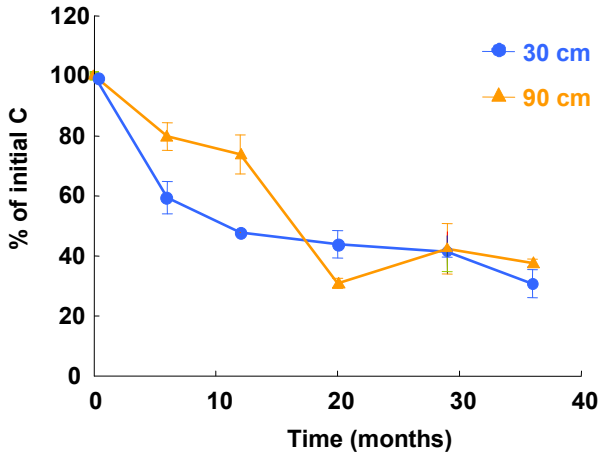

Fig. 6. Root litter remaining (% of initial C added) during the three years of incubation in 30 and 90 cm soil depth (data from Sanaullah et al., 2011).

fresh biomass may be more complete, thereby diminishing the formation of lignocellulosic compounds capable of sorption onto metal oxides. As a result stabilized OM may consist primarily of microbial cells. Thus, our study is consistent with the microbial efficiency-matrix stabilisation (MEMS) hypothesis recently postulated by Cotrufo et al. (2013), which says that microbial use efficiency determines stabilization through interaction with the mineral phase. Our results may indicate that microbial use efficiency could affect OM stabilization by incomplete degradation as well as formation of microbial material.

Acknowledgments

The study was funded by the European commission under the framework of the EXPEER project and by the ANR project DIMIMOS. We also thank the SOERE ACBB for providing the samples. The National NanoSIMS Facility at the Museum National d'Histoire Naturelle was established by funds from the CNRS, Région Île de France, Ministère délégué à l'Enseignement supérieur et à la Recherche, and the Muséum itself.

References

Balesdent, J., Petraud, J.P., Feller, C., 1991. Effets des ultrasons sur la distribution granulomètrique des matières organiques des sols. Science du sol 95–106.
Baldock, J.A., Oades, J.M., Nelson, P.N., Skene, T.M., Golchin, A., Clarke, P., 1997. Assessing the extent of decomposition of natural organic materials using solid-state 13C NMR spectroscopy. Australian Journal of Soil Research 35, 1061–1083.
Basile-Doelsch, I., Amundson, R., Stone, W.E.E., Borschneck, D., Bottero, J.Y., Moustier, S., Masin, F., Colin, F., 2007. Mineral control of carbon pools in a volcanic soil horizon. Geoderma 137, 477–489.
Baumann, K., Sanaullah, M., Chabbi, A., Dignac, M.-F., Bardoux, G., Steffens, M., Kögel-Knabner, I., Rumpel, C., 2013. Changes of litter chemistry and soil lignin signature during decomposition and stabilisation of 13C labelled wheat roots in three soil horizons. Soil Biology and Biochemistry 67, 55–61.
Chabbi, A., Kögel-Knabner, I., Rumpel, C., 2009. Stabilised carbon in subsoil horizons is located in spatially distinct parts of the soil profile. Soil Biology and Biochemistry 41, 256–271.
Cotrufo, M.F., Wallenstein, M.D., Boot, C., Denef, K., Paul, E., 2013. The microbial efficiency-matrix stabilisation (MEMS) framework integrates plant litter decomposition with soil organic matter stabilization: do labile plant inputs form stable organic matter? Global Change Biology 19, 988–995.
Dungait, J.A.J., Hopkins, D.W., Gregory, A.S., Whitmore, A.P., 2012. Soil organic matter turnover is governed by accessibility not recalcitrance. Global Change Biology 18, 1781–1796.
Eusterhues, K., Rumpel, C., Kleber, M., Kögel-Knabner, I., 2003. Stabilisation of soil organic matter by interactions with minerals as revealed by mineral dissolution and oxidative degradation. Organic Geochemistry 34, 1591–1600.
Fontaine, S., Barot, S., Barré, P., Bdioui, N., Mary, B., Rumpel, C., 2007. Stability of organic carbon in deep soil layers controlled by fresh carbon supply. Nature 450, 277–281.
Herrmann, A.M., Ritz, K., Nunan, N., Clode, P.L., Pett-Ridge, J., Kilburn, M.R., Murphy, D.V., O'Donnell, A.G., Stockdale, E.A., 2007. Nano-scale secondary ion mass spectrometry –a new analytical tool in biogeochemistry and soil ecology: a review article. Soil Biology and Biochemistry 39, 1835–1850.
Hernes, P.J., Kaiser, K., Dyda, R.Y., Cerli, C., 2013. Molecular trickery in soil organic matter: hidden lignin. Environmental Science and Technology 47, 9077–9085.
Kaiser, K., Zech, W., 1998. Dissolved organic matter sorption by mineral constituents of subsoil clay fractions. Plant Nutrition and Soil Science 163, 531–535.
Kleber, M., Sollins, P., Sutton, R., 2007. A conceptual model of organo-mineral interactions in soils: self assembly of organic molecular fragments into zonal structures on mineral surfaces. Biogeochemistry 85, 9–24.
Keiluweit, M., Bougoure, J.J., Zeglin, L.H., Myrold, D.D., Weber, P.K., Pett-Ridge, J., Kleber, M., Nico, P.S., 2012. Nano-scale investigation of the association of microbial nitrogen residues with iron (hydr)oxides in a forest soil O-horizon. Geochimica and Cosmochimica Acta 95, 213–226.
Kiem, R., Kögel-Knabner, I., 2003. Contribution of lignin and polysaccharides to the refractory carbon pool in C-depleted arable soils. Soil Biology and Biochemistry 35, 101–118.
Kleber, M., Mikutta, R., Torn, M.S., Jahn, R., 2005. Poorly crystalline mineral phases protect organic matter in acid subsoil horizons. European Journal of Soil Science 56, 717–725.
Kögel-Knabner, I., Guggenberger, G., Kleber, M., Kandeler, E., Kalbitz, K., Scheu, S., Eusterhues, K., Leinweber, P., 2008. Organo-mineral associaltions in temperate soils: integrating biology, mineralogy and organic matter chemistry. Journal of Plant Nutrition and Soil Science 171, 61–82.
Kramer, M.G., Sanderman, J., Chadwick, O.A., Chorover, J., Vitousek, P.M., 2012. Long-term carbon storage through retention of dissolved aromatic acids by reactive particles in soil. Global Change Biology 18, 2594–2605.
Liang, C., Balser, T.C., 2008. Preferential sequestration of microbial carbon in subsoils of a glacial-landscape toposequence, Dane County, WI, USA. Geoderma, 148, pp. 113–119.
Liu, X., Eusterhues, K., Thieme, J., Ciobota, V., Höschen, C., Mueller, C.W., Küsel, K., Kögel-Knabner, I., Rösch, P., Popp, J., Totsche, K.U., 2013. STXM and NanoSIMS investigations on EPS fractions before and after adsorption to goethite. Environmental Science and Technology 47, 3158–3166.
Miltner, A., Bombach, P., Schmidt-Brücken, B., Kästner, M., 2012. Som genesis: microbial biomass as a significant source. Biogeochemistry 111, 41–55.
Mayer, L.M., 1994. Relationship between mineral surfaces and organic carbon concentrations in soils and sediments. Chemical Geology 114, 347–363.
Mikutta, R., Zand, U., Chorover, J., Haumaier, L., Kalbitz, K., 2011. Stabilisation of extracellular polymeric substances (Bacillus subtilis) by adsorption to and coprecipitation with Al forms. Geochimica and Cosmochimica Acta 75, 3135–3154.
Mueller, C.W., Kölbl, A., Hoeschen, C., Hillion, F., Heister, K., Herrmann, A.M., Kögel-Knabner, I., 2012. Submicron scale imaging of soil organic matter dynamics using NanoSIMS – from single particles to intact aggregates. Organic Geochemistry 42, 1476–1488.
Moni, C., Chabbi, A., Nunan, N., Rumpel, C., Chenu, C., 2010. Spatial dependance of organic carbon-metal relationships. A multi-scale statistical analysis, from horizon to field. Geoderma 158, 120–127.
Ransom, B., Kim, D., Kastner, M., Wainwright, S., 1998. Organic matter preservation on continental slopes: importance of mineralogy and surface area. Geochimica et Cosmochimica Acta 62, 1329–1345.
Remusat, L., Hatton, P.J., Nico, P.S., Zeller, B., Kleber, M., Derrien, D., 2012. NanoSIMS study of organic matter associated with soil aggregates: advantages, limitations and combination with STXM. Environmental Science and Technology 46, 3943–3949.
Rumpel, C., Kögel-Knabner, I., 2011. Deep soil organic matter – a key but poorly understood component of terrestrial C cycle. Plant and Soil 338, 143–158.
Rumpel, C., Eusterhues, K., Kögel-Knabner, I., 2010. Non-cellulosic neutral sugar contribution to mineral associated organic matter in top-and subsoil horizons of two acid forest soils. Soil Biology and Biochemistry 42, 379–382.
Rumpel, C., Rodríguez-Rodríguez, A., González-Pérez, J.A., Arbelo, C., Chabbi, A., Nunan, N., González-Vila, F.J., 2012. Contrasting composition of mineralbound organic matter in top and subsoil horizons of Andosols. Biology and Fertility of Soils 48, 401–411.
Sanaullah, M., Chabbi, A., Leifeld, J., Bardoux, G., Billiou, D., Rumpel, C., 2011. Decomposition and stabilization of root litter in top- and subsoil horizons: what is the difference? Plant and Soil 338, 127–141.
Schmidt, M.W.I., Rumpel, C., Kögel-Knaber, I., 1999. Evaluation of an ultrasonic dispersion method to isolate primary organomineral complexes from soils. European Journal of Soil Science 50, 87–90.
Schrumpf, M., Kaiser, K., Guggenberger, G., Persson, T., Kögel-Knabner, I., Schulz, E.D., 2013. Storage and stability of organic carbon in soils as related to depth, occlusion within aggregates, and attachment to minerals. Biogeosciences 10, 1675–1691.
Spielvogel, S., Prietzel, J., Kögel-Knabner, I., 2008. Soil organic matter stabilisation in acidic forest soils is preferential ans soil type-specific. European Journal of Soil Science 59, 674–692.
Thomen, A., Robert, F., Remusat, L., 2014. Determination of the nitrogen abundance in organic materials by NanoSIMS quantitative imaging. Journal of Analytical Atomic Spectrometry 29, 512–519.
Vogel, C., Mueller, C.W., Höschen, C., Buegger, F., Heister, K., Schulz, S., Schloter, M., Kögel-Knabner, I., 2014. Submicron structures provide preferential spots for carbon and nitrogen sequestration in soils. Nature Communications 5, 2947.